

Quantum simulator for the Schwinger effect with atoms in bichromatic optical lattices

Nikodem Szpak* and Ralf Schützhold†

Fakultät für Physik, Universität Duisburg-Essen, Duisburg, Germany

(Received 25 March 2011; revised manuscript received 13 May 2011; published 22 November 2011)

Ultracold atoms in specifically designed optical lattices can be used to mimic the many-particle Hamiltonian (whose effective parameters can be tuned in a wide range) describing electrons and positrons in an external electric field. This analogy facilitates the experimental simulation of (so far unobserved) fundamental quantum phenomena such as the Schwinger effect, i.e., spontaneous electron-positron pair creation out of the vacuum by a strong electric field. Such an experiment would also test nonperturbative aspects of these lattice systems.

DOI: [10.1103/PhysRevA.84.050101](https://doi.org/10.1103/PhysRevA.84.050101)

PACS number(s): 03.65.Pm, 67.85.-d, 12.20.-m

Introduction. There are several fundamental predictions of relativistic quantum field theory which have so far eluded a direct experimental verification. One prominent example is the Schwinger [1] effect (historically more accurate would be the name Sauter-Schwinger effect—see Refs. [2] and [3]), i.e., the spontaneous creation of electron-positron pairs out of the vacuum by a strong electric field. For a constant electric field E , the leading-order e^+e^- pair creation probability scales as [1–3]

$$P_{e^+e^-} \sim \exp \left\{ -\pi \frac{c^3 M^2}{\hbar q E} \right\} = \exp \left\{ -\pi \frac{E_S}{E} \right\}, \quad (1)$$

where $E_S = M^2 c^3 / (\hbar q)$ is the critical field strength determined by the elementary charge q and the mass M of an electron (or positron). The above expression (1) for $P_{e^+e^-}$ does not permit a Taylor expansion in q , i.e., it is inherently nonperturbative and thus cannot be represented by any finite set of Feynman diagrams.

Unfortunately, our theoretical understanding of this nonperturbative quantum electrodynamics (QED) effect is still very incomplete. Apart from the constant field case, only very simple field configurations where the electric field either depends on time $E(t)$ or on one spatial coordinate such as $E(x)$ are fully solved [4]. For example, recently it has been found that the occurrence of two different frequency scales in a time-dependent field $E(t)$ can induce drastic changes in the (momentum-dependent) pair creation probability [5,6]. Moreover, the impact of interactions between the electron and the positron of the created pair, as well as between them and other electrons and positrons or photons, is not understood. This ignorance is unsatisfactory not only from a theoretical point of view but also in view of planned experiments which envisage field strengths not too far below the critical field strength E_S and thus could be able to probe this effect experimentally [7].

These considerations motivate the investigation of the Schwinger effect via a different line of approach. By suitably designing a laboratory system, we could reproduce the quantum many-particle Hamiltonian describing electrons and positrons in an electric field and thereby obtain a quantum simulator for the Schwinger effect. This would facilitate the

investigation of space-time-dependent electric fields such as $E(t, x)$ and should also provide some insight into the role of interactions. It should be stressed here that our proposal goes beyond the simulation of the (classical or first-quantized) Dirac equation on the single-particle level—see, e.g., Ref. [8]—but aims at the full quantum many-particle Hamiltonian. A correct description of many-body effects such as particle-hole creation (including the impact of interactions) requires creation and annihilation operators in second quantization. There are some proposals for the second-quantized Dirac Hamiltonian [9] but they consider scenarios which are more involved than the setup discussed here and aim at different models and effects. Similarly, the recent observation of Klein tunneling in graphene [10] deals with massless Dirac particles—but the mass gap is crucial¹ for the nonperturbative Schwinger effect [cf. Eq. (1)].

The model. We start with the Dirac equation [11] describing electrons and positrons propagating in an electromagnetic vector potential A_μ which are described by the spinor wave function Ψ ($\hbar = c = 1$)

$$\gamma^\mu (i \partial_\mu - q A_\mu) \Psi - M \Psi = 0. \quad (2)$$

For simplicity, we consider 1 + 1 dimensions ($\mu = 0, 1$) where the Dirac matrices γ^μ satisfying $\{\gamma^\mu, \gamma^\nu\} = 2\eta^{\mu\nu}$ can be represented by the Pauli matrices $\gamma^0 = \sigma_3$ and $\gamma^1 = -i\sigma_1$. Since in one spatial dimension there is no magnetic field we can choose the gauge $qA_0 = \Phi$ and $A_1 = 0$. As a result, the Dirac equation simplifies to $i\partial_t \Psi(t, x) = (-i\sigma_2 \partial_x + M\sigma_3 + \Phi) \Psi(t, x)$. In one spatial dimension, there is also no spin, hence the wave function has only two components $\Psi = (\Psi^1, \Psi^2)$. The Hamiltonian for the classical Dirac field then reads

$$H = \int dx \Psi^\dagger (-i\sigma_2 \partial_x + M\sigma_3 + \Phi) \Psi. \quad (3)$$

As the next step, we discretize the space dimension and introduce a regular grid (lattice) $x_n = na$ with a positive grid (lattice) constant a and integers $n \in \mathbb{Z}$. The discretization of the wave function $\Psi_n(t) := \sqrt{a} \Psi(t, x_n)$, defined now at

¹Even though one can create a mass gap in graphene via suitable interactions breaking the effective time-reversal symmetry, most of the other advantages of optical lattices (such as the ability to address and measure single sites, to control the parameters, and to switch the coupling on and off) do not apply to graphene in this way.

*nikodem.szpak@uni-due.de

†ralf.schuetzhold@uni-due.de

the grid points x_n , gives rise to a discretized derivative $\sqrt{a} \partial_x \Psi(t, x_n) \rightarrow [\Psi_{n+1}(t) - \Psi_{n-1}(t)]/(2a)$. Finally, replacing the x integral by a sum, we obtain

$$H \rightarrow \sum_n \Psi_n^\dagger \left[-\frac{i\sigma_2}{2a} (\Psi_{n+1} - \Psi_{n-1}) + M\sigma_3 \Psi_n + \Phi_n \Psi_n \right]. \quad (4)$$

In order to obtain the quantum many-body Hamiltonian, we quantize the discretized Dirac field operators via the fermionic anticommutation relations $\{\hat{\Psi}_n^\alpha, \hat{\Psi}_m^\beta\} = 0$ and $\{\hat{\Psi}_n^\alpha, [\hat{\Psi}_m^\beta]^\dagger\} = \delta_{nm} \delta^{\alpha\beta}$. Using $\hat{\Psi}_n = (\hat{a}_n, \hat{b}_n)$, i.e., $\hat{\Psi}_n^{\alpha=1} = \hat{a}_n$ and $\hat{\Psi}_n^{\alpha=2} = \hat{b}_n$, the discretized many-particle Hamiltonian reads

$$\hat{H} = \frac{1}{2a} \sum_n [\hat{b}_{n+1}^\dagger \hat{a}_n - \hat{b}_n^\dagger \hat{a}_{n+1} + \text{H.c.}] + \sum_n [(\Phi_n + M) \hat{a}_n^\dagger \hat{a}_n + (\Phi_n - M) \hat{b}_n^\dagger \hat{b}_n]. \quad (5)$$

The first term describes jumping between the neighboring grid points while the remaining two terms can be treated as a combination of external potentials. Due to the specific form of the jumping, the lattice splits into two disconnected sublattices: (A) containing \hat{a}_{2n} and \hat{b}_{2n+1} and (B) containing \hat{a}_{2n+1} and \hat{b}_{2n} with integers n . Since the two sublattices behave basically in the same way, it is sufficient to consider only one of them, say, A. Identifying $\hat{c}_{2n} = (-1)^n \hat{a}_{2n}$ and $\hat{c}_{2n+1} = (-1)^{n+1} \hat{b}_{2n+1}$, we obtain the form of the well-known Fermi-Hubbard Hamiltonian for a one-dimensional lattice

$$\hat{H} = -J \sum_n [\hat{c}_{n+1}^\dagger \hat{c}_n + \hat{c}_n^\dagger \hat{c}_{n+1}] + \sum_n V_n \hat{c}_n^\dagger \hat{c}_n, \quad (6)$$

with hopping rate $J = 1/(2a)$ and on-site potentials $V_{2n} = \Phi_{2n} + M$ and $V_{2n+1} = \Phi_{2n+1} - M$. This Hamiltonian will be the starting point for the design of the optical lattice analogy. But before we proceed, we note that the free part \hat{H}_0 of this Hamiltonian, i.e., with $\Phi_n = 0$, can be explicitly diagonalized. Performing a discrete Fourier transform on the lattice $\hat{a}_p := \sum_n e^{-2inap} \hat{a}_{2n}$ and $\hat{b}_p := \sum_n e^{-i(2n+1)ap} \hat{b}_{2n+1}$, for $p \in (-\pi/2a, \pi/2a)$ and introducing operators \hat{A}_p and \hat{B}_p , which diagonalize \hat{H}_0 , we obtain

$$\hat{H}_0 = \int dp E_p [\hat{A}_p^\dagger \hat{A}_p - \hat{B}_p^\dagger \hat{B}_p] \quad (7)$$

with the energy spectrum [where $J = 1/(2a)$]

$$E_p = \sqrt{M^2 + J^2 \cos^2(ap)}. \quad (8)$$

It approximates the relativistic energy-momentum relation at the edge of the Brillouin zone, for $p \approx \pm\pi/(2a)$. The spectrum of \hat{H}_0 consists thus of two symmetric intervals separated by a gap of $2M$. In order to obtain a positive Hamiltonian, we perform the usual redefinition $\hat{B}_p^\dagger \leftrightarrow \hat{B}_p$ which corresponds to changing the vacuum state by filling all \hat{B}_p states by a fermion. This is completely analogous to the *Dirac sea* picture in quantum electrodynamics. In terms of this analogy, \hat{A}_p^\dagger or \hat{A}_p create or annihilate an electron, whereas \hat{B}_p or \hat{B}_p^\dagger create or annihilate a hole in the *Dirac sea*—which is then a positron. An additional potential Φ_n , if sufficiently localized in space, will not modify this spectrum but may introduce

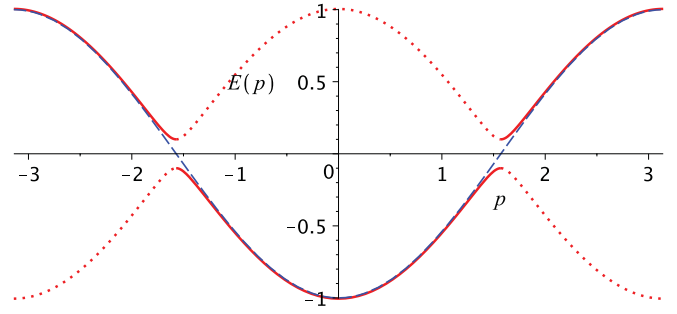


FIG. 1. (Color online) Sketch of the dispersion relation (in units of J and $1/a$) for $\Delta W = 0$ (dashed blue curve) and small $\Delta W > 0$ (solid and dotted red curves).

isolated eigenvalues with eigenstates corresponding to bound states localized in space.

Experimental setup. The Fermi-Hubbard Hamiltonian (6) can be realized with ultracold fermionic atoms in a one-dimensional optical lattice with the potential

$$W(x) = W_0 \sin^2(2kx) + \Delta W \sin^2(kx), \quad (9)$$

where $k = \pi/(2a)$, by taking $W_0 \gg \Delta W$ and adding a suitable deformation $\Phi(x)$ —see Fig. 2 below. Similar settings have already been obtained experimentally [12].

Although discretization of $W(x)$ at $x_n = na$ gives directly V_n of (6), the small perturbation ΔW doubles the original periodicity of the potential $W(x)$ and thus some mathematical caution in treating ΔW perturbatively is required. By a version of WKB approximation for periodic potentials [13], we rederive the Hubbard model and the energy band structure from first principles, using two sets of Wannier functions localized in the “upper” and the “lower” minima of the potential $W(x)$, respectively. An interesting universal phenomenon occurs—see Fig. 1. For $\Delta W = 0$, the lowest band is described, in the *nearest-neighbor approximation* used here, by $E_p = -J \cos(ap)$ (the dashed blue curve in Fig. 1). Switching on a small $\Delta W > 0$, which immediately doubles the period of the potential, forces the energy dispersion relation to halve its period (the Brillouin zone shrinks by a factor of 2) while keeping a similar functional dependence on p when $\Delta W \ll W_0$. It leads to splitting of this band into two subbands (red solid and dotted curves in Fig. 1) which are approximately described by (8). Thus the nearest-neighbor approximation reproduces relation (8) for $J = 1/(2a)$ and holds uniformly for all values of the quasimomentum p as long as ΔW and J are small [14]. In the vicinity of the minimum of the upper band and the maximum of the lower band, separated by a gap $2M \approx \Delta W$, it reproduces the relativistic energy-momentum relation. The corresponding Hamiltonian has the same form as the one for the discretized Dirac equation (7), thus completing the analogy.

Using again the WKB approximation, we find that the hopping rate $J \approx 4\sqrt{W_0 E_R} \exp\{-\pi\sqrt{W_0/E_R}/4\}/\pi$ is mainly determined by the potential strength W_0 , the laser wave number k , and the mass m_{atom} of the atoms (not to be confused with the effective mass M of the Dirac particles to be simulated), where $E_R = k^2/(2m_{\text{atom}}) = \pi^2/(8m_{\text{atom}}a^2)$ is the recoil energy. The correction ΔW generates the mass gap $M \approx \Delta W/2$.

The analog of the e^+e^- pair creation can be simulated if the involved scales obey the hierarchy

$$\omega_{\text{osc}} \gg J \gg M \gg T. \quad (10)$$

First, the local oscillator frequency ω_{osc} in the potential minima must be larger than J to ensure the applicability of the single-band Fermi-Hubbard Hamiltonian (6). Second, $J \gg M$ is required for the continuum limit, i.e., that the discretized expression (4) provides a good approximation. Similarly, the change $\Delta\Phi_n = \Phi_{n+1} - \Phi_n$ of the analog of the electrostatic potential Φ_n from one site to the next should be much smaller than M . Over many sites, however, this change can well exceed the mass gap $2M$, which is basically one of the conditions for the Schwinger effect to occur. Finally, the effective temperature T should be well below the mass gap $2M$ in order to avoid thermal excitations. For example, ${}^6\text{Li}$ atoms in an optical lattice made of light with a wavelength of 500 nm would have a recoil energy E_R of $\sim 7 \mu\text{K}$. If we choose the potential strength as $W_0 = 10 \mu\text{K}$, the hopping rate J would be $\sim 5 \mu\text{K}$, which is still sufficiently below the local oscillator frequency ω_{osc} of $\sim 34 \mu\text{K}$. With $\Delta W = 1 \mu\text{K}$ we would get a mass M of 500 nK and the effective temperature should be below that value. While the generation of such optical lattices with these parameters is experimentally state of the art (see, e.g., Ref. [12]), achieving the required low temperatures is probably the major experimental challenge.

Bose-Fermi mapping. Since it is typically easier to cool down bosonic than fermionic atoms, let us discuss an alternative realization based on bosons in an optical lattice. They are described by the Bose-Hubbard Hamiltonian which has the same form as (6) after replacing the fermionic \hat{c}_n by bosonic \hat{d}_n operators, but with an additional on-site repulsion term $U(\hat{d}_n^\dagger \hat{d}_n - 1)\hat{d}_n^\dagger \hat{d}_n$. For large $U \gg J$, we obtain the bosonic analog of ‘‘Pauli blocking,’’ i.e., at most one particle can occupy each site. Neglecting all states with double or higher occupancy, we can map these bosons exactly onto fermions in one spatial dimension via

$$\hat{c}_n = \hat{d}_n \prod_{m < n} \exp(-i\pi \hat{d}_m^\dagger \hat{d}_m). \quad (11)$$

As a result, we obtain the same physics as described by the Fermi-Hubbard Hamiltonian (6).

Simulation procedure. The above established analogy between the (discretized) quantum many-particle Hamiltonian of electrons and positrons in an electric field and the (Bose or Fermi) Hubbard model describing ultracold atoms in optical lattices facilitates laboratory simulations of relativistic phenomena of strong-field QED. Probably the most prominent of them is the spontaneous pair creation in strong electric fields known also as the Schwinger effect [1–3] which has to date not been confirmed experimentally, to the best of our knowledge. The original Schwinger effect [1] deals with a constant electric field E and would correspond to a static tilted optical lattice with $\Phi(x) = Ex$. However, in view of the planned experiments [7], an electric field which is localized in space and time is more realistic. In order to clearly distinguish nonperturbative spontaneous pair creation (via tunneling) from other perturbative effects such as dynamical pair creation, the electric field should be slowly varying [4,15].

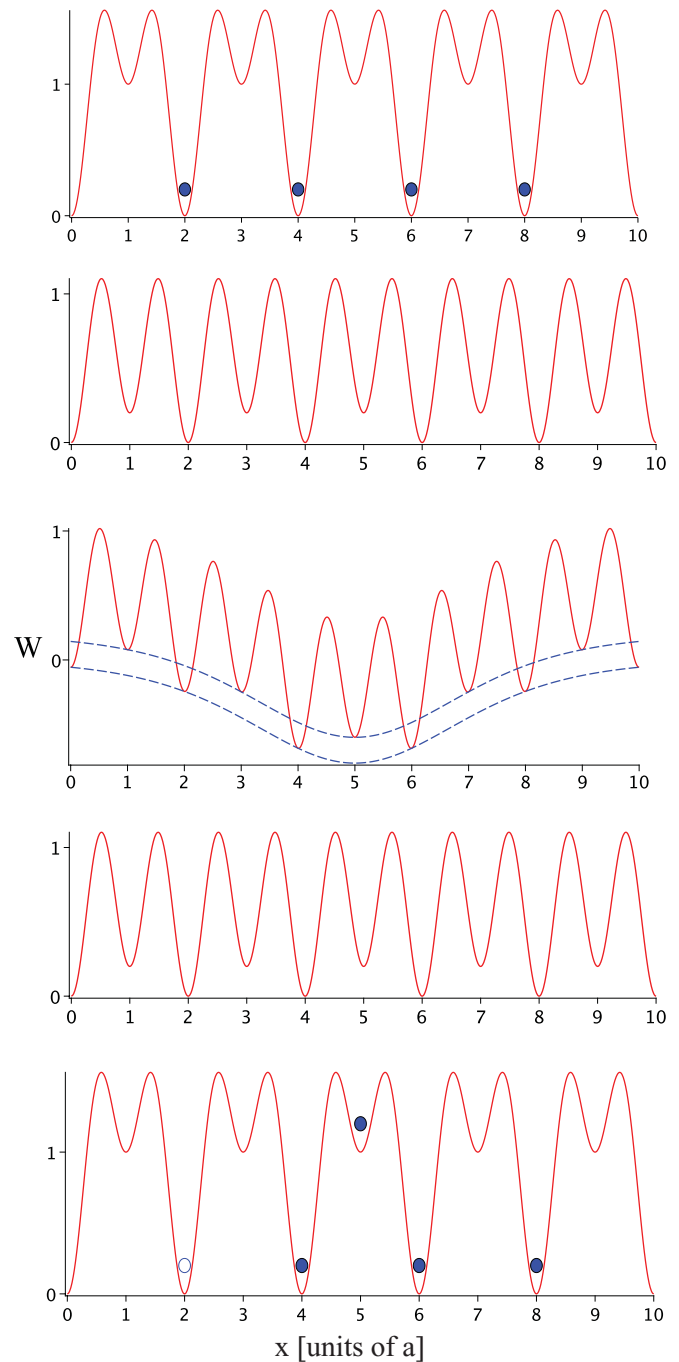


FIG. 2. (Color online) Sketch (not to scale) of the temporal stages of the simulation (from top to bottom). Plotted are the optical lattice potential $W(x)$ (solid red curves) and the effective electric potential $\Phi(x)$ (dashed blue curves). The blue solid (empty) dots represent particles (holes).

As a result, we envisage an experimental realization sketched in Fig. 2. In order to prepare the initial state, we start with $\Delta W \gg W_0$, where the two bands are separated by a large gap. The *Dirac sea* then corresponds to the state where all lower minima are filled with atoms while all upper minima are empty (half filling of the lattice—see the first picture in Fig. 2). If we then decrease ΔW adiabatically until $\Delta W \ll W_0$ and thus $J \gg M$, the atoms become delocalized—but still

the lower band is filled while the upper band remains empty (the second picture in Fig. 2). As the next stage, we slowly switch on an additional potential Φ to facilitate tunneling from the lower band to the upper band—the analog of the Schwinger effect (the third picture in Fig. 2). Finally, after slowly switching off the potential Φ again (the fourth picture in Fig. 2), we increase ΔW adiabatically until $\Delta W \gg W_0$. By this energetic separation, a particle-hole pair created via tunneling is transformed to an atom in one of the upper minima and, consequently, a missing atom (i.e., hole) in one of the lower minima (the fifth picture in Fig. 2). This could be detected by site-resolved imaging [16], for example.

Note that the creation of a particle-hole pair separated by $2n$ lattice sites requires the simultaneous tunneling of n particles (at half filling) since two particles cannot occupy the same site. Describing this process via simple perturbation theory in terms of the hopping Hamiltonian $J\hat{c}_{m+1}^\dagger\hat{c}_m$ (i.e., in powers of J), the probability P_n for n -particle tunneling scales with the n th power of the single-particle tunneling probability. In order to overcome the band gap ΔW , the minimum number $2n$ of lattice sites is inversely proportional to the lattice tilt $\Delta\Phi = \Phi_{n+1} - \Phi_n$, i.e., the analog of the electric field E . Thus we observe the same exponential scaling $\ln(P_n) \sim -\Delta W/\Delta\Phi$ as

in Eq. (1) showing that this process is nonperturbative in $\Delta\Phi$. Turning this argument around, the analogy to QED can help us to understand the nonperturbative properties of Hubbard lattice Hamiltonians. This again emphasizes the many-particle character of our proposal which goes beyond the simulation of the classical Dirac equation. Apart from investigating the pair creation probability for space-time-dependent electric fields $E(t, x)$, this quantum simulator for the Schwinger effect could provide some insight into the impact of interactions. In the case of dipolar interactions between the atoms, we would get the coupling Hamiltonian $D_{nm}\hat{c}_n^\dagger\hat{c}_m^\dagger\hat{c}_n\hat{c}_m$ with $D_{nm} \propto |n - m|^{-3}$. For example, the interaction energy D_{nm} due to the large magnetic moments of ^{52}Cr atoms would be below one nK. Larger interaction energies up to a few μK can be obtained for ^6Li atoms by external electric fields of order 10^8 V/m which induce electric dipole moments [17]. By aligning the atomic dipole moments parallel or perpendicular to the lattice, we may even switch between attractive $D_{nm} < 0$ and repulsive $D_{nm} > 0$ interactions.

R. S. acknowledges stimulating discussions during the Benasque Workshop on *Quantum Simulations* in 2011 and financial support from the DFG (SFB-TR12).

-
- [1] J. Schwinger, *Phys. Rev.* **82**, 664 (1951).
 [2] F. Sauter, *Z. Phys.* **69**, 742 (1931); **73**, 547 (1931).
 [3] W. Heisenberg and H. Euler, *Z. Phys.* **98**, 714 (1936); V. Weisskopf, *Kong. Dans. Vid. Selsk., Math.-fys. Medd.* **XIV**, 6 (1936); reprinted in: J. Schwinger (ed.), *Quantum Electrodynamics* (Dover, New York, 1958).
 [4] See, e.g., A. I. Nikishov and V. I. Ritus, *Sov. Phys. JETP* **25**, 1135 (1967); E. Brezin and C. Itzykson, *Phys. Rev. D* **2**, 1191 (1970); F. V. Bunkin and I. I. Tugov, *Sov. Phys. Dokl.* **14**, 678 (1970); N. B. Narozhnyi and A. I. Nikishov, *Sov. J. Nucl. Phys.* **11**, 596 (1970); V. S. Popov, *JETP Lett.* **13**, 185 (1971); **18**, 255 (1973); S. P. Kim and D. N. Page, *Phys. Rev. D* **65**, 105002 (2002); V. S. Popov, *JETP Lett.* **75**, 045013 (2007); N. B. Narozhny, S. S. Bulanov, V. D. Mur, and V. S. Popov, *Phys. Lett. A* **330**, 1 (2004); V. S. Popov, *JETP Lett.* **80**, 382 (2004); H. Gies and K. Klingmüller, *Phys. Rev. D* **72**, 065001 (2005); G. V. Dunne and C. Schubert, *ibid.* **72**, 105004 (2005); H. K. Avetissian, A. K. Avetissian, G. F. Mkrtchian, and Kh. V. Sedrakian, *Phys. Rev. E* **66**, 016502 (2002); H. K. Avetissian, *Relativistic Nonlinear Electrodynamics* (Springer, New York, 2006).
 [5] R. Schützhold, H. Gies, and G. Dunne, *Phys. Rev. Lett.* **101**, 130404 (2008); G. V. Dunne, H. Gies, and R. Schützhold, *Phys. Rev. D* **80**, 111301 (2009).
 [6] C. K. Dumlu and G. V. Dunne, *Phys. Rev. Lett.* **104**, 250402 (2010).
 [7] See, e.g., the European ELI programme: [<http://www.extreme-light-infrastructure.eu/>].
 [8] Witthaut *et al.*, e-print arXiv:1102.4047; W. G. Unruh and R. Schützhold, *Phys. Rev. D* **68**, 024008 (2003); S. Longhi, *Phys. Rev. A* **81**, 022118 (2010); F. Dreisow, M. Heinrich, R. Keil, A. Tunnermann, S. Nolte, S. Longhi, and A. Szameit, *Phys. Rev. Lett.* **105**, 143902 (2010); R. Gerritsma, B. P. Lanyon, G. Kirchmair, F. Zähringer, C. Hempel, J. Casanova, J. J. Garcia-Ripoll, E. Solano, R. Blatt, and C. F. Roos, *ibid.* **106**, 060503 (2011); R. Gerritsma *et al.*, *Nature (London)* **463**, 68 (2010); L. Lamata, J. León, T. Schätz, and E. Solano, *Phys. Rev. Lett.* **98**, 253005 (2007).
 [9] J. I. Cirac, P. Maraner, and J. K. Pachos, *Phys. Rev. Lett.* **105**, 190403 (2010); S.-L. Zhu, B. Wang, and L.-M. Duan, *ibid.* **98**, 260402 (2007); J.-M. Hou, W.-X. Yang, and X.-J. Liu, *Phys. Rev. A* **79**, 043621 (2009); L.-K. Lim, C. M. Smith, and A. Hemmerich, *Phys. Rev. Lett.* **100**, 130402 (2008); O. Boada, A. Celi, J. I. Latorre, and M. Lewenstein, *New J. Phys.* **13**, 035002 (2011); N. Goldman, A. Kubasiak, A. Bermudez, P. Gaspard, M. Lewenstein, and M. A. Martin-Delgado, *Phys. Rev. Lett.* **103**, 035301 (2009).
 [10] K. S. Novoselov *et al.*, *Nature (London)* **438**, 197 (2005); M. I. Katsnelson, K. S. Novoselov, and A. K. Geim, *Nat. Phys.* **2**, 620 (2006); D. Allor, T. D. Cohen, and D. A. McGady, *Phys. Rev. D* **78**, 096009 (2008); B. Dora and R. Moessner, *Phys. Rev. B* **81**, 165431 (2010); B. Rosenstein, M. Lewkowicz, H. C. Kao, and Y. Korniyenko, *ibid.* **81**, 041416(R) (2010); H. C. Kao, M. Lewkowicz, and B. Rosenstein, *ibid.* **82**, 035406 (2010).
 [11] P. A. M. Dirac, *Proc. R. Soc. (London) A* **117**, 610 (1928); **118**, 351 (1928); **126**, 360 (1930).
 [12] T. Salger, C. Geckeler, S. Kling, and M. Weitz, *Phys. Rev. Lett.* **99**, 190405 (2007).
 [13] N. L. Balazs, *Ann. Phys.* **53**, 421 (1969).
 [14] N. Szpak and R. Schützhold, e-print arXiv:1109.2426 (to appear in *New J. Phys.*).
 [15] N. Szpak, *J. Phys. A* **41**, 164059 (2008); Ph.D. thesis, Frankfurt am Main, 2006; P. Pickl and D. Dürr, *Europhys. Lett.* **81**, 40001 (2008).
 [16] J. F. Sherson *et al.*, *Nature (London)* **467**, 68 (2010).
 [17] M. Marinescu and L. You, *Phys. Rev. Lett.* **81**, 4596 (1998).